Journal of Southeast University (English Edition) Vol. 27, No. 3, pp. 284 – 289 Sept. 2011 ISSN 1003—7985

Effect of secondary pore distribution on adsorption diffusion performance of n-hexane on 5A zeolite pellets

Du Xudong Liu Zongjian Cui Qun Wang Haiyan Yao Huqing

(College of Chemistry and Chemical Engineering, Nanjing University of Technology, Nanjing 210009, China)

Abstract: Adsorption rates of n-hexane on the 5A zeolite at 100 to 300 ℃ and 0.01 to 10 kPa are determined by an intelligent gravimetric analyzer (IGA-100), and the adsorption diffusion performance of n-hexane on 5A zeolite pellets with different secondary pore distributions is analyzed. The results indicate that 5A-1 and 5A-6 zeolites have similar micropore and mesopore size distribution, while the 5A-6 zeolite has a larger secondary pore volume when the pore diameter is between 0.1 and 1 μm and more secondary pores when the pore diameter is less than 0.01 μm. The effective diffusion coefficient of n-hexane on the 5A-6 zeolite pellet is 10^{-6} to 10^{-4} cm^2/s, about 2 to 5 times higher than that on the 5A-1 zeolite. The effective diffusion coefficient of n-hexane on the 5A-1 zeolite pellet improves from 5×10^{-7} to 2×10^{-6} cm^2/s when the temperature increases from 100 to 300 ℃. However, the effective diffusion coefficient of n-hexane on the 5A-6 zeolite remains almost unchanged at different temperatures. The molecular average free path of n-hexane decreases from 627.15-963.28 to 0.63-0.96 μm with the adsorption pressure increasing from 0.01 to 10 kPa. Such a free path is close to the secondary pore diameter, resulting in significant Knudsen diffusion in the secondary pores. Thus, the effective diffusion coefficient of n-hexane on the 5A zeolite pellets increases before 1 kPa and decreases after 1 kPa.

Key words: 5A zeolite; pore structure; secondary pore; diffusion; n-hexane

doi: 10.3969/j.issn.1003 – 7985.2011.03.012

As a typical non-polar solvent, n-hexane has been widely used as an extracting agent, a diluent agent of medical synthesis, and an advanced solvent. In particular, high purity n-hexane (mass content ≥ 98.5%) is an attractive material for developments in biochemistry, pharmacentics and so on [1–4]. Generally, n-hexane can be obtained from straight-chain gasoline, the condensate of natural gas, raffinate oil or pyrolysis gasoline. Meanwhile, the remaining isoparaffins, after n-hexane has been abstracted, are also good additives for the octane improvement of gasoline pools[5]. However, it is impractical to separate n-hexane from its isomers thoroughly using conventional methods like distillation owing to their close boiling points. Adsorption separation has been proven to be a promising approach in segregating iso/normal paraffins by means of molecule fingerprinting with 5A zeolite employment, leading to an effective utilization of petroleum naphtha and value-added products [5–8]. However, using such a technique to produce high purity n-hexane or other single normal paraffins is still not feasible in China. In previous studies, we successfully established a method of separating n-hexane from industrial hexane and C6 mixture[9–11] and evaluated the performance of various adsorbents upon iso/normal paraffins severance [12–14].

For the industrial application of 5A zeolite on iso/normal paraffins separation, the adsorbents are prepared as particulated zeolite containing small microporous crystals inside macroporous pellets. The adsorbents generally offer two distinct resistances against the mass transfer: the secondary pore resistance of the pellet and the microporous resistance of the crystals [15–18], which gives rise to the complication in the diffusion of adsorption and interferes with the sieving effect of adsorbents, adsorption/desorption rate, etc. [6–7, 15–18]. Furthermore, the effect of the secondary pore on the diffusivity of n-hexane on 5A zeolite pellets has rarely been reported.

Therefore, this paper investigates the effects of different secondary pores distribution, adsorption temperature and pressure on effective diffusivity performance of n-hexane on 5A zeolite pellets by IGA.

1 Materials and Methods

1.1 Materials

The adsorbents are binder-free 5A zeolites differentiated at secondary pores and bulk properties (see Tab.1). The particle size is −10 to +14 US standard mesh. The particle density and porosity are determined by a mercury intrusion porosimetry (MIP). The crystallite dimension is analyzed by a scanning electron microscope (SEM), and the amount of calcium cation exchange is measured by X-ray fluorescence (XRF). The n-hexane is of 99% purity, purchased from Sinopharm Chemical Reagent Co., Ltd., Shanghai, China.

Tab.1 Bulk properties of the used 5A zeolite

Property	5A-1	5A-6
Bulk density/($g \cdot cm^{-3}$)	0.79	0.73
Particle density/($g \cdot cm^{-3}$)	1.25	1.19
Porosity ε_p	26.19	29.26
Crystallite dimension/μm	2.2	2.2
Amount of calcium cation exchange/%	78	78

1.2 Characterization

The BET specific surface area, the micropore size distribution, and the volume of the micropore are calculated by the BET equation and the HK equation, which are based on carbon dioxide adsorption isotherms at 0 ℃[19] by a Micromeritics ASAP 2020 surface area and porosimetry analyzer.

The BJH specific surface area, the mesopore size distribution and the volume of the mesopore are calculated by the

Received 2011-05-27.

Biographies: Du Xudong (1984—), male, graduate; Cui Qun (corresponding author), female, doctor, professor, cuiqun@njut.edu.cn.

Foundation item: The National Natural Science Foundation of China (No. 20876074).

Citation: Du Xudong, Liu Zongjian, Cui Qun, et al. Effect of secondary pore distribution on adsorption diffusion performance of n-hexane on 5A zeolite pellets[J]. Journal of Southeast University (English Edition), 2011, 27(3): 284 – 289. [doi: 10.3969/j.issn.1003 – 7985.2011.03.012]

BJH method from nitrogen adsorption isotherms at liquid nitrogen temperature by a Micromeritics ASAP 2020.

The porosity and macropore size distribution of the 5A zeolite are measured by mercury (Poremaster GT-60).

1.3 Theory of adsorption kinetics

The adsorption rate curves of n-hexane on 5A zeolite (100 to 300 ℃, 0 to 12 kPa) are measured by an intelligent gravimetric analyzer (IGA-100, HIDEN ISOCHEMA, UK). Prior to measuring, the zeolite sample is activated by heating from ambient temperature to 400 ℃ at 0.1 Pa for 12 h.

2 Results and Discussion

2.1 Porous structure of 5A zeolites

Figs. 1 to 4 show the micropore, the mesopore, the secondary pore size distribution and the secondary pore number fraction of 5A zeolites in sequence. Tab. 2 summarizes the specific surface areas and the pore volumes of 5A zeolites.

5A-1 and 5A-6 zeolites have similar micropore and mesopore size distributions, as shown in Figs. 1 and 2. Since the amount of calcium cation exchange is about 78%, 5A-1 and 5A-6 zeolites have a uniform pore size distribution between 0.42 to 0.56 nm (see Fig. 1). Considering the crystal defects and gaps between crystals, 5A-1 and 5A-6 zeolites also have pore sizes greater than 0.6 nm, enabling the promotion of the diffusion of n-hexane in 5A zeolites. Tab. 2 shows that 5A-1 and 5A-6 zeolites have a similar micropore BET surface area of about 590 m^2/g and the pore volume of about 0.24 cm^3/g. From Fig. 2, we can see that 5A-1 and 5A-6 zeolites only have a few mesopores from 2.5 to 4.0 nm. As listed in Tab. 2, the mesopore volumes of 5A zeolites are from 0.063 2 to 0.069 1 cm^3/g.

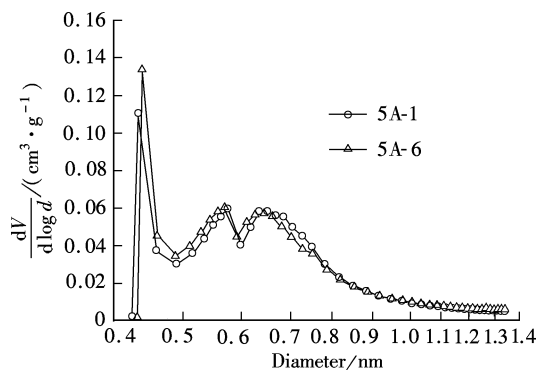

Fig. 1 Micropore distribution of 5A zeolites

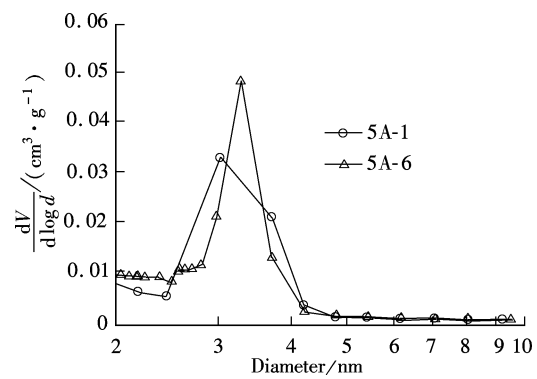

Fig. 2 Mesopore distribution of 5A zeolites

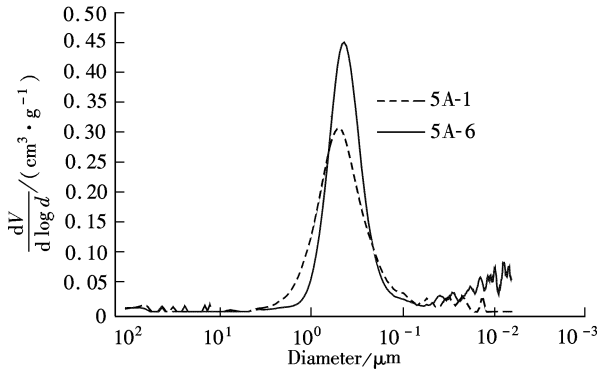

Fig. 3 Secondary pore distribution of 5A zeolites

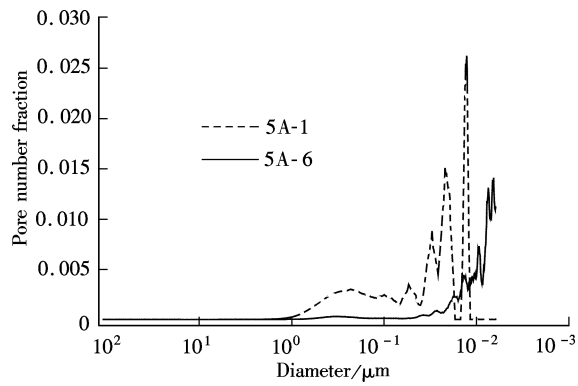

Fig. 4 Secondary pore number fraction of 5A zeolites

Tab. 2 Pore volume, diameter and specific surface area of 5A zeolites

Pore structure parameters		5A-1 zeolite	5A-6 zeolite
Micropore (<2 nm)	BET surface area/($m^2 \cdot g^{-1}$)	585.336 2	593.494 3
	Pore volume/($cm^3 \cdot g^{-1}$)	0.242 7	0.246 1
Mesopore (2 to 50 nm)	BJH surface area/($m^2 \cdot g^{-1}$)	64.504 0	69.457 0
	Pore volume/($cm^3 \cdot g^{-1}$)	0.069 1	0.063 2
Macropore (>50 nm)	Surface area/($m^2 \cdot g^{-1}$)	1.321	2.211
	Pore volume/($cm^3 \cdot g^{-1}$)	0.173	0.211
	Porosity/%	26.190	29.260

Fig. 3 and Tab. 2 show the differences of the secondary pore distribution between 5A-1 zeolites and 5A-6 zeolites. The 5A-6 zeolite has a secondary pore surface area and a pore volume of 2.211 m^2/g and 0.211 cm^3/g, respectively, while those of the 5A-1 zeolite are 1.321 m^2/g and 0.171 cm^3/g, respectively. Fig. 4 indicates that the 5A-6 zeolite has a large amount of pores less than 0.01 μm, despite the fact that the size of 0.1 to 1 μm provides a larger secondary pore volume. The secondary pores of the 5A-1 zeolite are mainly distributed between 0.01 to 0.1 μm, and no portion of less than 0.01 μm is observed.

2.2 Adsorption rate curve of n-hexane on 5A zeolite

The adsorption rate curves of n-hexane on 5A-1 and 5A-6 zeolites at 100 to 300℃ measured by IGA-100 are presented in Figs. 5 and 6.

Fig. 5 shows that, under low coverage, the adsorption rate of n-hexane on the 5A-6 zeolite is higher than that of 5A-1 at 100 ℃. When the temperature increases from 200

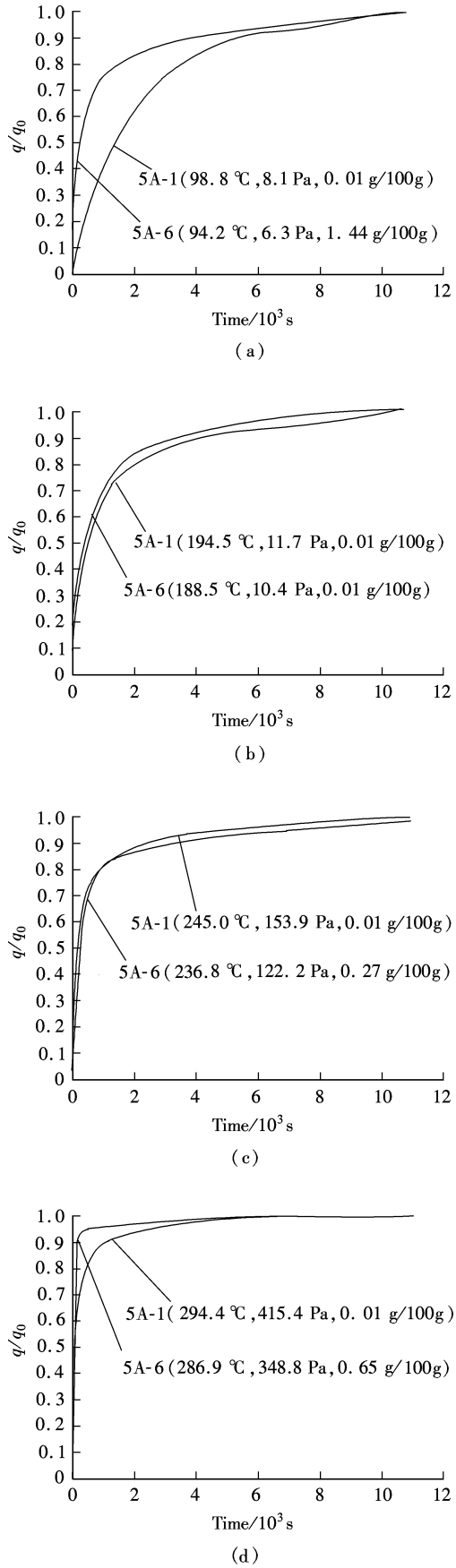

Fig. 5 Adsorption rate curves of n-hexane on 5A zeolites under low coverage. (a) 100 ℃; (b) 200 ℃; (c) 250 ℃; (d) 300 ℃

to 300 ℃, the adsorption rates become analogical to each other. This indicates that the major factor to n-hexane diffusion on the 5A zeolite is due to the difference of secondary pore size distribution at low temperatures. But at a higher temperature, the molecular thermal motion will be intensified. As a result, the diffusion of n-hexane on 5A-1

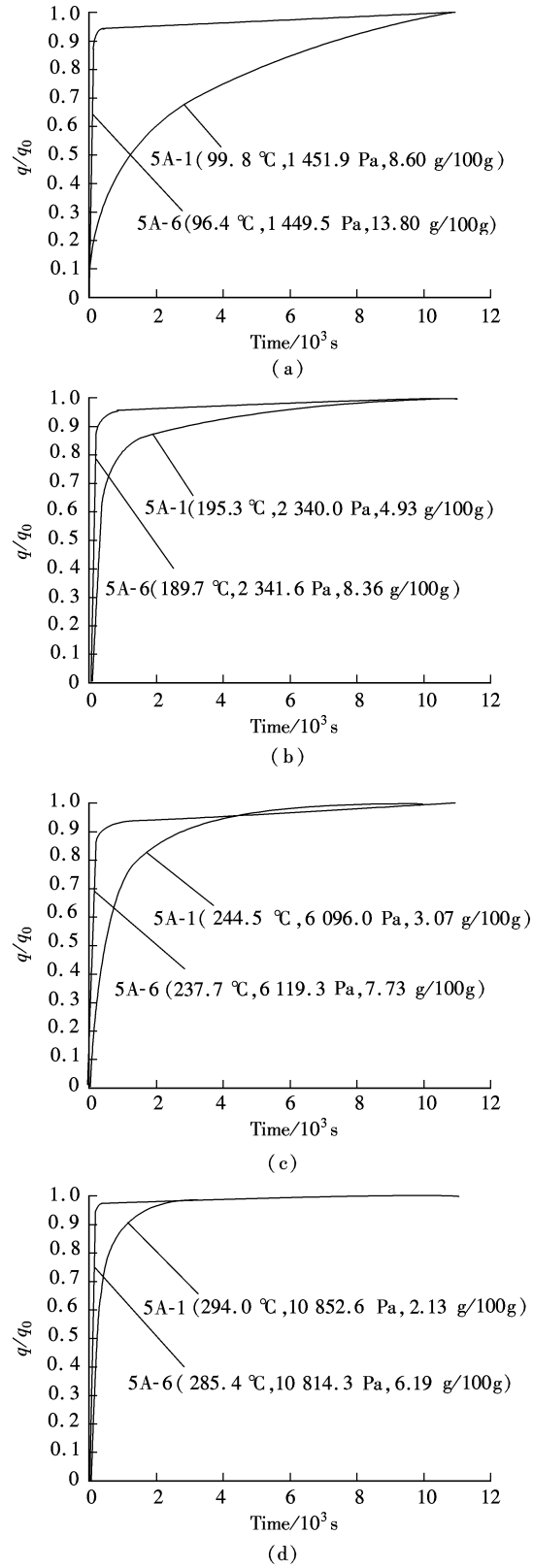

Fig. 6 Adsorption rate curves of n-hexane on 5A zeolites under high coverage. (a) 100 ℃; (b) 200 ℃; (c) 250 ℃; (d) 300 ℃

and 5A-6 zeolites mainly depends on the surface property and the micropore structure of the adsorbents.

Fig. 6 shows the adsorption rate curves of n-hexane on 5A-1 and 5A-6 zeolites under high coverage, indicating that the diffusion properties are related to the secondary pore structure. The adsorption rate of n-hexane on the 5A-6 zeolite is higher than that of n-hexane on the 5A-1 zeolite at the range of 100 to 300 ℃, owing to the larger secondary pore volume and more secondary pores of the 5A-6 zeolite.

2.3 Effective diffusivity coefficient of n-hexane on 5A zeolite

According to the adsorption rates of n-hexane on 5A-1 and 5A-6 zeolites at 100 to 300 ℃, the effective diffusivity coefficients of n-hexane on 5A-1 and 5A-6 zeolite pellets are calculated by[20-21]

$$\frac{m_t}{m_\infty} = \frac{6}{\sqrt{\pi}}\left(\frac{D_e}{R_p^2}t\right)^{1/2} \tag{1}$$

where t is the time, s; m_t is the mass adsorbed at time t, g/100 g; m_∞ is the mass adsorbed as $t\to\infty$, g/100 g; D_e is the effective diffusivity, cm^2/s; R_p is the adsorbent pellet radius, cm. The curves of the effective diffusion coefficients of n-hexane on 5A-1 and 5A-6 zeolites at 100 to 300 ℃ are shown in Fig. 7.

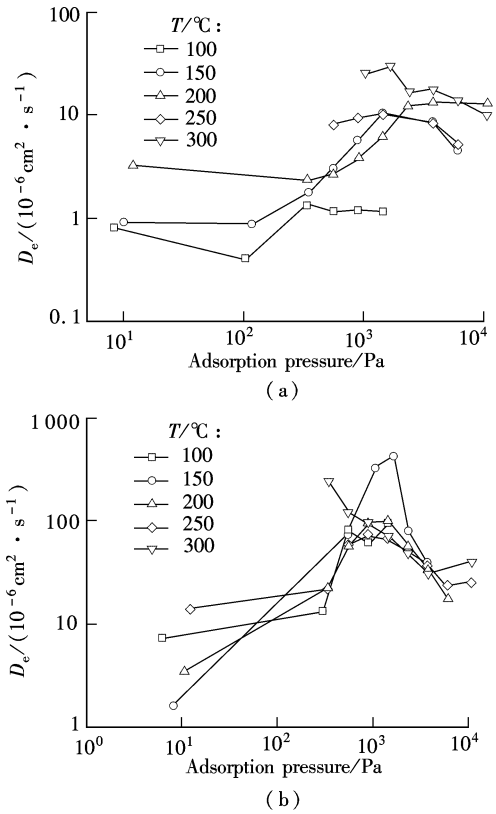

Fig. 7 Effective diffusion coefficients of n-hexane on 5A-1 and 5A-6 zeolites at 100 to 300 ℃. (a) 5A-1 zeolite; (b) 5A-6 zeolite

Fig. 7 shows that the adsorption pressure significantly influences the effective diffusivity coefficient of n-hexane on 5A-1 and 5A-6 zeolites under conditions of 100 to 300 ℃ and 0.01 to 10 kPa. At 0.01 kPa, the 5A-1 zeolite is similar to the 5A-6 zeolite in terms of the effective diffusivity coefficient which is related to the surface properties of the 5A zeolite at the low pressure. In addition, the effective diffusivity coefficient of n-hexane on the 5A-6 zeolite is 10^{-6} to 10^{-4} cm^2/s at 100 to 300 ℃ and 0.01 to 10 kPa, which is almost 2 to 5 times higher than that on the 5A-1 zeolite.

2.3.1 Effect of temperature on effective diffusivity coefficient

Fig. 7(a) reveals that the effective diffusivity coefficient of n-hexane on the 5A-1 zeolite is 2×10^{-5} cm^2/s at 300 ℃, about 10 times higher than that at 100℃. However, the effect of the effective diffusivity coefficient on the 5A-1 zeolite is not distinguished at 100 to 300 ℃ and 0.01 to 10 kPa, as shown in Fig. 7(b). With the increase in temperature, the thermal motion of the n-hexane molecule intensifies so as to enhance the diffusion of n-hexane on 5A-1 zeolite. The 5A-6 zeolite has more pathways for mass transfer due to the secondary pores, so the effect of thermal motion of the n-hexane molecule is not significant.

2.3.2 Influence of free path of n-hexane molecule on effective diffusivity coefficient

Tab. 3 shows the Maxwell free path of n-hexane at different temperatures and pressures calculated by

$$l = \frac{\kappa T}{\sqrt{2}\pi\sigma^2 p} \tag{2}$$

where p is the adsorption pressure, Pa; l is the mean free path of gas molecules, m; κ is the Boltzmann constant, $\kappa = 1.380\,66\times10^{-23}$ J/K; σ is the effective molecular diameter, m.

Tab. 3 Mean free path of n-hexane molecule μm

Pressure/kPa	100 ℃	150 ℃	200 ℃	250 ℃	300 ℃
0.01	627.15	711.18	795.21	879.25	963.28
1	6.27	7.11	7.95	8.79	9.63
2	3.14	3.56	3.98	4.40	4.82
10	0.63	0.71	0.80	0.88	0.96

The mean free path of the n-hexane molecule increases from 6.27 to 9.63 μm under the same pressure at 100 to 300 ℃, while it decreases rapidly from 6.27-9.63 μm to 0.63-0.96 μm when the pressure increases from 1 to 10 kPa. The results suggest that the pressure plays a more important role in determining the mean free path.

With the increase in the adsorption pressure, the effective diffusivity coefficient of n-hexane on 5A-1 and 5A-6 zeolites first increases and then decreases at 1 kPa, as shown in Fig. 7. From Figs. 3 and 4 and Tab. 3, it is observed that with the increase in the pressure, the mean free path of the n-hexane molecule decreases immediately till it reaches the level of secondary pore size, enlarging the Knudsen diffusion of the n-hexane molecule in the secondary pore of the 5A zeolite. For example, when the pressure is 0.01 kPa, the mean free path of the n-hexane molecule is about 627.15 to 963.28 μm, as shown in Tab. 3, which is similar to the distance of the gaps between zeolite pellets. The mean free path is then influenced by the diffusion of n-hexane zeolite pellets. When the pressure increases to 1 kPa, the mean free path of n-hexane decreases rapidly to 6.27 to 9.63 μm, which is much smaller than the distance between zeolite pellets but much greater than the size of the seconda-

ry pores inside the 5A zeolite, as shown in Fig. 3. So the effective diffusivity coefficients of n-hexane on 5A-1 and 5A-6 zeolites reach 10^{-5} and 10^{-4} cm^2/s, respectively. When the pressure increases to 2 kPa, the mean free path of n-hexane decreases to 3.14 to 4.82 μm, close to the size of the secondary pores, resulting in enhanced Knudsen diffusion. Both the effective diffusivity coefficients of 5A-1 and 5A-6 zeolites are maintained to be 10^{-5} and 10^{-4} cm^2/s, respectively. When the adsorption pressure is 10 kPa, the mean free path of n-hexane becomes 0.63 to 0.96 μm, and the effective diffusivity coefficient begins to decrease, especially for the 5A-6 zeolite. Due to the large amount of secondary pores less than 0.8 μm, the Knudsen diffusion of n-hexane on the 5A-6 zeolite is further consolidated and the effective diffusivity coefficient of n-hexane on the 5A-6 zeolite decreases to 10^{-5} cm^2/s. There are fewer secondary pores smaller than 0.1 μm on 5A-1 zeolite, especially for the size of pores smaller than 0.01 μm. Thus, there is a slight effect of the Knudsen diffusion of n-hexane on the 5A-1 zeolite between 2 and 10 kPa.

3 Conclusions

The effect of secondary pore distribution on adsorption diffusion of n-hexane on 5A zeolite pellets is investigated. The important findings are shown as follows:

1) 5A-1 and 5A-6 zeolites have similar micropore and mesopore size distributions, while the 5A-6 zeolite has larger secondary pore volume of less than 0.01 μm and more secondary pores between 0.1 and 1 μm.

2) The diffusion of n-hexane on the 5A zeolite is related to the surface property and the micropore structure of adsorbents under low coverage, but the adsorption diffusion performance is controlled by the secondary pore distribution under high coverage.

3) The effective diffusion coefficient of n-hexane on the 5A-6 zeolite pellet is from 10^{-6} to 10^{-4} cm^2/s under the conditions of temperatures of 100 to 300 ℃ and pressures of 0.01 to 10 kPa, which is about 2 to 5 times higher than that of the 5A-1 zeolite.

4) The effective diffusivity coefficient of n-hexane on the 5A-1 zeolite is 2×10^{-5} cm^2/s at 300 ℃, about 10 times higher than that at 100 ℃. The effect of temperature on diffusion of n-hexane over the 5A-6 zeolite is not significant.

5) The molecular average free path of n-hexane decreases from 627.15-963.28 to 0.63-0.96 μm with the increase in adsorption pressure from 0.01 to 10 kPa. The decreased free path enhances the Knudsen diffusion in the secondary pores. Thus, the effective diffusion coefficient of n-hexane on the 5A zeolite pellets increases before 1 kPa and decreases after 1 kPa.

This study provides critical data for designing special adsorbents and provides a practical application in the separation of iso/normal paraffins.

References

[1] Zhao L X, Ma Y, Sun L, et al. Research progress in theory and equipment for hexane production and purification [J]. *Modern Chemical Industry*, 2009, **29**(9): 15 - 22. (in Chinese)

[2] Wu R D, Ma F, Liu W Z, et al. Research on new environment-friendly solvent oil and the production technology [J]. *Shanghai Chemical Industry*, 2008, **33**(11): 26 - 30. (in Chinese)

[3] Wang Y W, Liu X X. Production and market status of solvent oils [J]. *Techno-Economics in Petrochemicals*, 2004, **19**(1): 43 - 46. (in Chinese)

[4] Wang Y F, Xing J X. Status quo and development trends of petroleum hydrocarbon solvent oils [J]. *Petroleum Refinery Engineering*, 2002, **32**(10): 44 - 47. (in Chinese)

[5] Bárcia P S, Silva J, Rodrigues A E. Separation by fixed-bed adsorption of hexane isomers in zeolite BETA pellets [J]. *Ind Eng Chem Res*, 2006, **45**(12): 4316 - 4328.

[6] Silca J, Rodrigues A E. Equilibrium and kinetics of n-hexane adsorption in pellets of 5A zeolite [J]. *AIChE Journal*, 1997, **43**(10): 2524 - 2534.

[7] Shen B X, Sun H. Adsorption kinetics of n-pentane and n-hexane on binder-free 5A molecular sieve [J]. *Petrochemical Technology*, 2008, **37**(8): 805 - 809. (in Chinese)

[8] Bárcia P S, Silva J, Rodrigues A E. Adsorption equilibrium and kinetics of branched hexane isomers in pellets of BETA zeolite [J]. *Microporous and Mesoporous Materials*, 2005, **79**(1/2/3): 145 - 163.

[9] Lu C, Du X D, Yao X L, et al. Study on breakthrough curves of industrial hexane in fixed-bed absorber containing 5A molecular sieves [J]. *Natural Gas Chemical Industry*, 2010, **35**(3): 30 - 34; 46. (in Chinese)

[10] Cui Q, Liu Z J, Du X D, et al. Process for producing n-heptane and n-octane simultaneously by pressure-swing adsorption: China, ZL200710133497.4 [P]. 2008-03-05. (in Chinese)

[11] Yao X L, Cui Q, Zhou L J, et al. Pressure-swing adsorption process for extraction of high-purity n-hexane: China, ZL200710133498.9[P]. 2008-03-26. (in Chinese)

[12] Yao X L, Du X D, Liu Z J, et al. Adsorption performance for n-hexane and characterization of 5A molecular sieves[J]. *Petrochemical Technology*, 2010, **39**(7): 757 - 761. (in Chinese)

[13] Yao X L, Du X D, Liu Z J, et al. Adsorption/desorption and diffusion performance of n-hexane on 5A zeolite at high temperature[J]. *Chemical Engineering*, 2010, **38**(11): 1 - 4. (in Chinese)

[14] Kang Y F, Du X D, Liu Z J, et al. Adsorption/desorption and diffusion property of n-hexane on 5A molecular sieves under high temperature [J]. *Journal of Chemical Engineering of Chinese Universities*, 2011, **25**(1): 172 - 176. (in Chinese)

[15] Shams K, Mirmohammadi S J. Preparation of 5A zeolite monolith granular extrudates using kaolin: investigation of the effect of binder on sieving/adsorption properties using a mixture of linear and branched paraffin hydrocarbons [J]. *Microporous and Mesoporous Materials*, 2007, **106**(1/2/3): 268 - 277.

[16] Chen S Z, Chang K Y, Bai Z L. Study on secondary pore in zeolite molecular sieve materials: Ⅰ. secondary pore in crystalline particle and equivalent diameter of crystalline particle [J]. *Journal of East China Institute of Chemical Technology*, 1990, **16**(6): 611 - 617. (in Chinese)

[17] Bai Z L, Chen S Z, Chang K Y, et al. Study on secondary pores in zeolite molecular sieve materials: Ⅱ. effect of intracrystalline secondary pores of Y type zeolite on diffusion [J]. *Journal of East China Institute of Chemical Technology*, 1993, **19**(3): 249 - 254. (in Chinese)

[18] He J, Yan A Z. Studies on properties of 5A molecular sieve for dewaxing processes: Ⅳ. influence of Ca^{2+} exchange degree on desorption and diffusion of n-paraffins in CaNaA molecular sieves [J]. *Acta Petrolei Sinica*, 1995, **11**(3): 13 - 20. (in Chinese)

[19] Gil A, Gandía L M. Microstructure and quantitative estimation of the micropore-size distribution of an alumina-pillared clay from nitrogen adsorption at 77 K and carbon dioxide adsorption at 273 K [J]. *Chemical Engineering Science*, 2003, **58**: 3059 - 3075.
[20] Ruthven D M. *Principles of adsorption and adsorption processes* [M]. New York: Wiley, 1984.
[21] Karger J, Ruthven D M. *Diffusion in zeolites and other microporous solids* [M]. New York: Wiley, 1992.

二次孔分布对正己烷在5A分子筛颗粒上吸附扩散性能的影响

杜旭东　刘宗健　崔　群　王海燕　姚虎卿

（南京工业大学化学化工学院，南京 210009）

摘要：采用 IGA－100 型智能重力分析仪测定在 100～300 ℃，0.01～10 kPa 下，5A 分子筛对正己烷的吸附速率曲线，分析了不同二次孔分布的成型 5A 分子筛颗粒 5A-1 和 5A-6 对正己烷的吸附扩散性能. 结果表明：5A-1 与 5A-6 分子筛具有相近的微孔和中孔孔径分布；5A-6 分子筛在孔径 0.1～1 μm 范围内拥有相对更大的二次孔孔容，而在孔径小于 0.01 μm 时拥有更丰富的二次孔分布；丰富的二次孔分布使得正己烷在 5A-6 分子筛上的有效扩散系数 D_e 为 10^{-6}～10^{-4} cm^2/s，是 5A-1 分子筛的 2～5 倍；随着吸附温度从 100 ℃增大至 300 ℃，5A-1 分子筛上的有效扩散系数从 5×10^{-7}～2×10^{-6} cm^2/s 增大至 2×10^{-5} cm^2/s，而在 5A-6 分子筛上的有效扩散系数随着吸附温度变化不明显；吸附压力从 0.01 kPa 升高至 10 kPa，引起正己烷分子平均自由程从 627.15～963.28 μm 下降至 0.63～0.96 μm，并与分子筛二次孔孔径相当，引起 Knudsen 扩散加剧，从而使正己烷在 5A 分子筛上的有效扩散系数于压力 1 kPa 前后呈现先上升后下降的变化趋势.

关键词：5A 沸石；孔结构；二次孔；扩散；正己烷

中图分类号：TQ028.15；TQ424.25